

ICONN 2015 [4<sup>th</sup> -6<sup>th</sup> Feb 2015]  
International Conference on Nanoscience and Nanotechnology-2015  
SRM University, Chennai, India

## Effect of annealing on tin oxide nanoparticles and vanadium-tin oxide nanocomposites prepared using sol-gel method

S. Mohana Priya, A. Geetha\* and K. Ramamurthi

Department of Physics and Nanotechnology, SRM University,  
Kattankulathur, Chennai 603203.

**Abstract:** Tin oxide, a wide band gap semiconductor material, is having wide range of applications. Tin oxide nanoparticles and vanadium-tin oxide mixed nanocomposites were synthesized by sol gel method using tin chloride and ammonium metavanadate as starting materials. Ammonia solution was added dropwise in the 0.3 M of tin chloride solution to synthesize tin oxide nanoparticles. 0.1 M (and 0.2 M) of ammonium metavanadate solution and 0.3 M tin chloride solutions were mixed together and the ammonia solution was added dropwise in the solution to prepare vanadium-tin oxide mixed nanocomposites. The synthesized SnO<sub>2</sub> nanoparticles and V-SnO<sub>2</sub> nanocomposites were annealed at 400°C and characterized by X-ray diffraction, scanning electron microscopic, energy dispersive X-ray and UV-Vis spectroscopic studies. The crystallite size of the synthesized nanoparticles and nanocomposites was derived from X-ray diffraction peaks using Debye-Scherrer formula. Surface morphology of tin oxide nanoparticles and vanadium-tin oxide nanocomposites was analyzed by scanning electron microscopic study.

**Keywords:** nanocomposites, tin oxide, vanadium oxide, sol-gel method.

### Introduction

In the recent years, nanocomposites occupy a major part of research. Nanocomposites are multiphase materials, formed by mixing two or more materials<sup>1</sup>. Hence they exhibit different nanostructures and properties suitable for application in various fields<sup>2</sup>. Among the various nanocrystalline materials tin oxide plays a major role in sensor application due to its wide band gap energy of 3.6 eV<sup>3,4</sup>. It is an n-type semiconductor material and finds application in the fields like solar cells, liquid crystal displays, optoelectronic devices<sup>5</sup> and gas sensing applications<sup>6</sup>. Generally the band gap increases, when the size of the particle decreases less than a significant size, since decrease in particle size increases the surface-volume ratio where excitons are created<sup>7</sup>. Vanadium oxide is a transition metal oxide which has several oxidation states like V<sup>3+</sup> to V<sup>5+</sup><sup>8</sup>. Vanadium oxide exists in the VO, VO<sub>2</sub>, VO<sub>3</sub>, V<sub>2</sub>O<sub>3</sub> and V<sub>2</sub>O<sub>5</sub> phases and is useful for several applications<sup>9</sup>, mainly V<sub>2</sub>O<sub>5</sub> as a catalyst<sup>8</sup>. There are various synthesis methods available to prepare nanocomposites. They are sol gel<sup>10</sup>, solvothermal<sup>3</sup>, microwave<sup>11</sup>, co-precipitation<sup>12</sup> and hydrothermal methods<sup>13</sup>. In the present work, the sol gel method was employed to prepare the pure tin oxide nanoparticles and vanadium-tin oxide nanocomposites. This method is simple, cost effective and the yield is relatively more. Sol-gel method is an effective method to prepare materials for gas sensor applications due to its low temperature treatment<sup>14</sup>. Preparation of Au/V-SnO<sub>2</sub> nanocomposites<sup>15</sup>, V-SnO<sub>2</sub> nanoparticles<sup>13</sup>, nanocrystalline Au:Ag:SnO<sub>2</sub> films<sup>5</sup> and

synthesis and characterization of indium-tin oxide nanoparticles<sup>16</sup> were reported. Wang et al.<sup>13</sup> used ammonium hydroxide as the stabilizing agent and prepared V-SnO<sub>2</sub> (vanadium-tin oxide) nanocomposites. In the present work SnO<sub>2</sub> nanoparticles and vanadium tin oxide nanocomposites were synthesized and characterized by X-ray diffraction, scanning electron microscopy, energy dispersive X-rays and UV –Vis spectroscopy techniques.

## Experimental

### Preparation of SnO<sub>2</sub> nanoparticles and V-SnO<sub>2</sub> nanocomposites:

Chemicals used in this work were purchased from Merck with 99.9% purity of Analytical Reagent. Tin chloride (SnCl<sub>2</sub>.2H<sub>2</sub>O) and ammonium metavanadate (NH<sub>4</sub>VO<sub>3</sub>) were the precursors used to prepare SnO<sub>2</sub> nanoparticles and V-SnO<sub>2</sub> nanocomposites. Tin oxide nanoparticles and vanadium-tin oxide nanocomposites were synthesized using sol-gel method. 0.3 M of SnCl<sub>2</sub>.2H<sub>2</sub>O solution was prepared using ethanol. The solution was stirred adding ammonia solution drop wise to make the solution with pH 8. The product was centrifuged and then dried in oven at 60°C<sup>10</sup>. V-SnO<sub>2</sub> nanocomposites were prepared from two different molar ratios of the solution. Tin chloride and ammonium metavanadate precursors were used to prepare nanocomposites by sol gel method following the process used to prepare the pure SnO<sub>2</sub> nanoparticles discussed above. The colour of pure SnO<sub>2</sub> nanopowder is ash when vanadium is added, the colour of V-SnO<sub>2</sub> nanopowders becomes olive green. The obtained product was calcined at 400°C for two hours and characterized for their structural, optical and surface morphological properties. X-ray diffraction pattern (XRD) of the samples were recorded using X-ray diffractometer (X'Pert PAN Analytical) with CuK $\alpha$  radiation ( $\lambda=1.5405\text{\AA}$ ). Morphological studies were carried out using scanning electron microscope attached with EDAX-COXEM TM 200. Optical properties were studied using UV-Vis Spectrophotometer (Shimadzu 2450).

## Results and discussion

### Structural Studies:

#### Pure SnO<sub>2</sub> nanoparticles:

Fig.1 shows the XRD pattern of the SnO<sub>2</sub> nanoparticles prepared following sol-gel method. The XRD peaks were indexed as (110), (101), (200), (211), (220), (112), (301), (202) and (321) planes<sup>10</sup> by comparing with the JCPDS file (card No: 41-1445) which shows the formation of SnO<sub>2</sub> nanoparticles of tetragonal system. The lattice parameters calculated are  $a=4.73\text{\AA}$  and  $c=3.16\text{\AA}$  using the equation  $1/d^2 = (4\sin^2\theta)/\lambda^2 = (h^2/k^2)/a^2 + l^2/c^2$ . From the XRD peak, the SnO<sub>2</sub> average crystallite size of particles was calculated from Debye Scherer formula,  $D= 0.9\lambda/(\beta\cos\theta)$ , where  $\lambda$  is the wavelength of X-rays used ( $1.5405\text{\AA}$ ),  $\beta$  is the Full Width Half Maximum (FWHM) in radian and  $\theta$  is the angle of diffraction. The calculated average crystallite size from the XRD peaks of (110), (101) and (211) for a pure SnO<sub>2</sub> nanoparticles was 16.5nm.

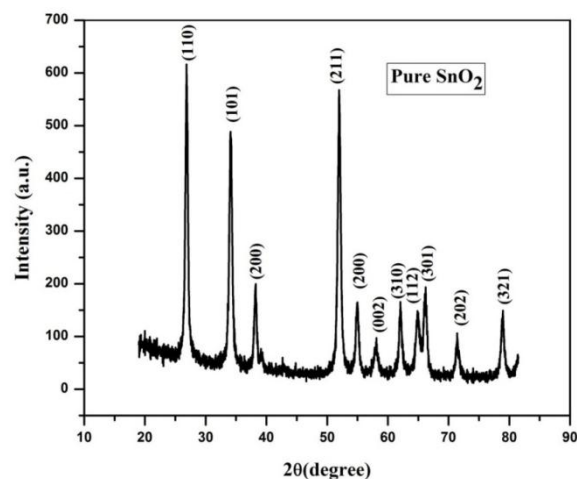
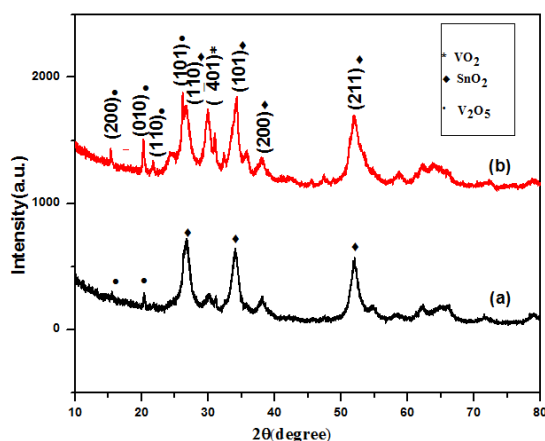


Fig.1 XRD pattern of SnO<sub>2</sub> nanoparticles.

### Vanadium-tin oxide nanocomposites

Fig.2 shows the XRD pattern of vanadium- tin oxide nanocomposites synthesized from different molar ratios of V/Sn [(0.1/0.3 and 0.2/0.3) M] and annealed at 400°C. XRD peaks (200)<sup>\*</sup>, (010)<sup>\*</sup> and (110)<sup>\*</sup> of V-SnO<sub>2</sub> confirm the formation of V<sub>2</sub>O<sub>5</sub> phase which belongs to orthorhombic crystal structure by comparing the peaks with the JCPDS file (No: 72-0598). When ammonium metavanadate is added to the SnCl<sub>2</sub> solution the intensity of (110)<sup>\*</sup> peak of SnO<sub>2</sub> decreases. On increasing more concentration of ammonium metavanadate in SnCl<sub>2</sub> solution the intensity of (110)<sup>\*</sup> peak is further decreased. Calculation shows that addition of ammonium metavanadate in the solution [(0.1/0.3) M] decreases the intensity of (110) peak of SnO<sub>2</sub> (fig. 2) and reduces the crystallite size of SnO<sub>2</sub> from 17.60nm to 5.72nm. Further increasing ammonium metavanadate concentration [(0.2/0.3) M] in the solution decreases the intensity of (110)<sup>\*</sup> XRD peak of SnO<sub>2</sub> (fig.2) and reduces the crystallite size of SnO<sub>2</sub> from 17.6 nm to 4.35nm. It is reported that increase in vanadium concentration in the solution decreases the crystallite size of the tin oxide in the V-SnO<sub>2</sub> nanoparticles annealed at 500°C<sup>12</sup>.



**Fig.2 XRD pattern of (a) 0.1/0.3 M and (b) 0.2/0.3 M of V-SnO<sub>2</sub> nanocomposites.**

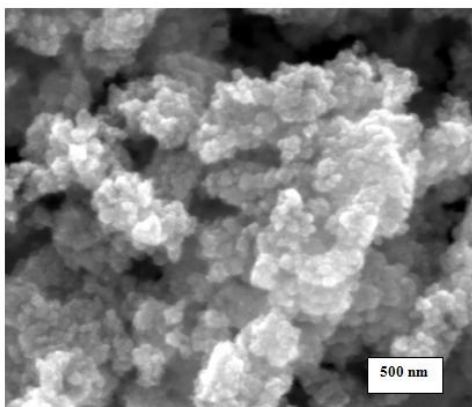
The XRD peaks of the synthesized SnO<sub>2</sub> material details are listed in the Table 1. The (0.2/0.3) M ratio solution gives, a peak at an angle of  $2\theta=26.2^\circ$  due to (101) plane which matches with the JCPDS file (No: 72-0598). Low concentration of vanadium, gives observed V<sub>2</sub>O<sub>5</sub> phase and when concentration of vanadium is increased. The XRD pattern exhibits the (401)<sup>\*</sup> peak at  $2\theta=30.0^\circ$  which is due to VO<sub>2</sub> phase of monoclinic system. Thus increase in the concentration of vanadium results in the formation of mixed phases of V<sub>2</sub>O<sub>5</sub> and VO<sub>2</sub>. The average crystallite size of vanadium- tin oxide nanocomposites synthesized from (0.1/0.3) M and (0.2/0.3) M solution calculated from (110), (101) and (211) XRD peaks using Debye Scherrer formula is respectively 7.6nm and 6.6nm.

**Table 1: hkl, FWHM, crystallite size(D), d-spacing values of SnO<sub>2</sub> XRD pattern**

Sample	hkl	FWHM (in radians)	D (nm)	d-spacing
SnO <sub>2</sub>	(110)	0.4641	17.60	3.32
	(101)	0.5164	16.09	2.63
	(211)	0.5615	15.73	1.76
V-SnO <sub>2</sub> (0.1/0.3 M)	(110)	1.4271	5.72	3.32
	(101)	0.9655	8.61	2.63
	(211)	1.0225	8.62	1.76
V-SnO <sub>2</sub> (0.2/0.3 M)	(110)	1.8760	4.35	3.33
	(101)	1.0177	8.17	2.61
	(211)	1.2337	7.16	1.76

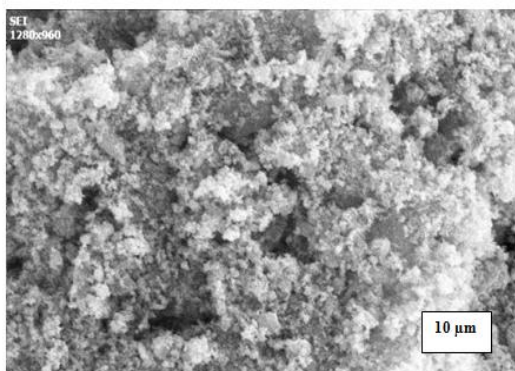
### Morphology analysis

Fig.3 shows the SEM images of pure tin oxide nanoparticles annealed at 400°C. It shows agglomerated spherical nanoparticles uniformly distributed on the surface.

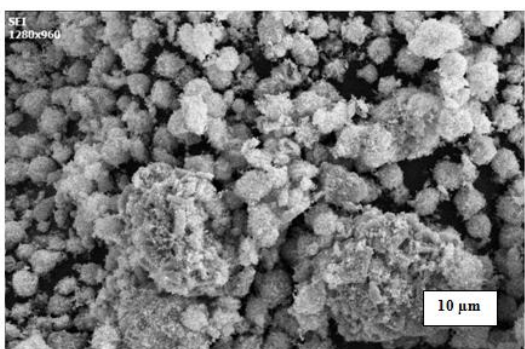


**Fig.3 SEM image of pure SnO<sub>2</sub> nanoparticles 0.3 M (calcinated at 400°C).**

Fig.4a shows the size of the agglomeration of the nanocomposites prepared from (0.1/0.3) M ratio. Fig.4b shows nearly spherical shaped agglomeration of V-SnO<sub>2</sub> nanocomposites prepared from (0.2/0.3)M ratio. Thus, the SEM images show that increasing ammonium metavanadate concentration in the solution effectively modifies the surface morphology of the synthesized V-SnO<sub>2</sub> nanocomposites.



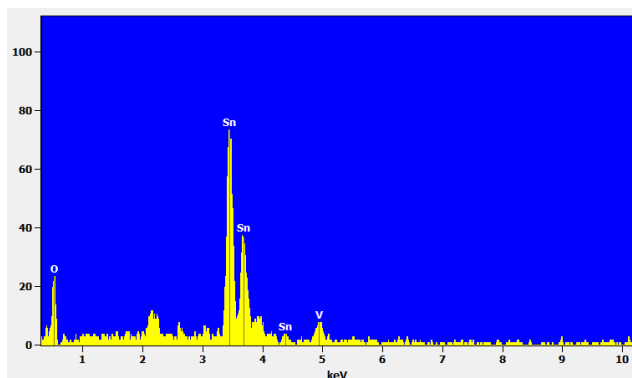
**Fig. 4a SEM image for (0.1/0.3 M) of V-SnO<sub>2</sub> nanocomposites (calcinated at 400°C).**



**Fig.4b SEM image for (0.2/0.3) M of V-SnO<sub>2</sub> nanocomposites shows coral reef like structure (calcinated at 400°C).**

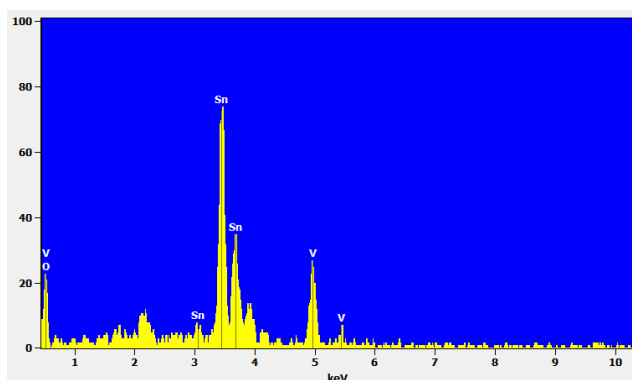
### EDAX Analysis

Fig.5a,b show the energy dispersive X-ray analysis (EDAX) of V-SnO<sub>2</sub> nanocomposites prepared from (0.1/0.3)M and (0.2/0.3)M solutions. It exhibits the clear peaks of tin, vanadium and oxygen elements, and no additional peaks were present which shows that it is excluded from the impurities of starting precursors.



**Fig .5a Elemental analysis for 0.1/0.3 M of V- SnO<sub>2</sub> nanocomposites for ratio.**

On increasing the vanadium concentration the percentage of tin present in the nanocomposites is decreased. The atomic percentage of Sn is 51.99%, V is 3.71% an O is 44.29%. When vanadium concentration is increased the percentage of Sn gets decreased to 48.45% and V is increased to 10.48% and O is decreased to 41.07% which is close to the stoichiometry compound.



**Fig.5b Elemental analysis for 0.2/0.3 M of V-SnO<sub>2</sub> nanocomposites.**

### Optical Properties

The band gap energy ( $E_g$ ) of the nanoparticles was calculated using the formula,  $\alpha hv = B( hv - E_g)^n$ , where  $n$  takes the value of  $\frac{1}{2}$  and  $2$  for direct and indirect transition respectively,  $B$  is a constant called band tailing parameter and  $hv$  is the incident photon energy. The Tauc's plot drawn between  $(\alpha hv)^2$  and  $hv$  is used to evaluate the  $E_g$ . Fig.6 shows the UV –Vis absorption spectrum of pure SnO<sub>2</sub> nanoparticles. The UV Visible absorption spectrum indicates a blue shift from the bulk SnO<sub>2</sub> (340nm). The band gap value of SnO<sub>2</sub> nanoparticles calculated using Tauc's plot is ~3.7eV which is larger than the bulk value of 3.6 eV. Fig.7 shows the UV-Vis absorption spectrum of V-SnO<sub>2</sub> nanocomposites. The band gap energy of V-SnO<sub>2</sub> nanocomposite calculated is 3.8 eV which is slightly larger than that of the pure SnO<sub>2</sub> nanoparticles. Further one can notice from this work that the band gap increases with decrease in crystallite size.

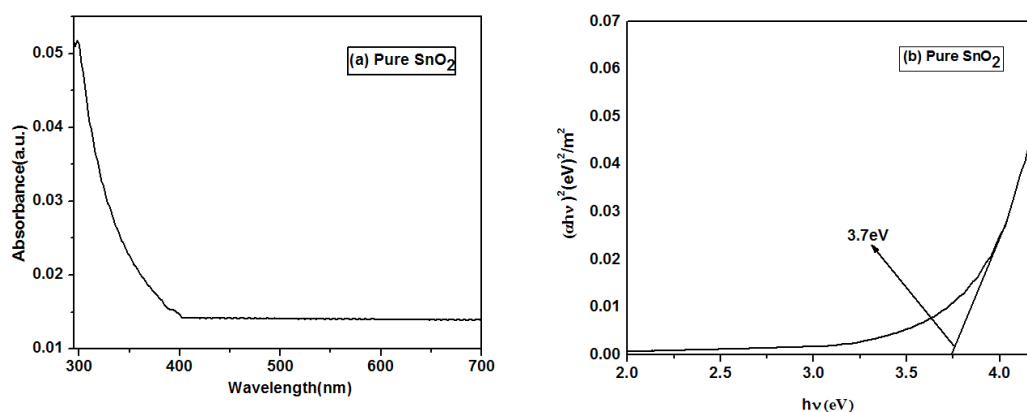


**Fig.6 (a) UV –Vis absorption spectrum for 0.3 M of pure SnO<sub>2</sub> nanoparticles and (b) band gap of SnO<sub>2</sub> nanoparticles.**

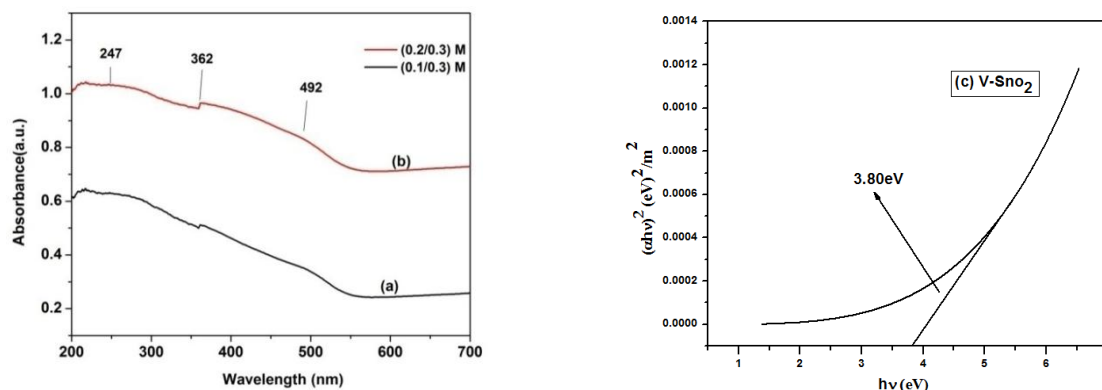


**Fig.7 UV –Vis absorption spectrum of V-SnO<sub>2</sub> nanocomposites (a) 0.1/0.3 M and (b) 0.2/0.3 M solution and (c) band gap of V-SnO<sub>2</sub> composites**

Fig. 7a shows the absorption band at 247nm in V-SnO<sub>2</sub> nanocomposites is due to O<sup>2-</sup>→V charge transfer transition and, the absorption band at 362nm is due to the V-O-V bridge<sup>17</sup> and the band at 492 is assigned to O<sup>2-</sup>→V<sup>5+</sup> charge transfer in an octahedral vanadium<sup>18</sup>, which indicates formation of mixed phases of vanadium. The band gap energy of V-SnO<sub>2</sub> nanocomposites is 3.8 eV (Fig. 7c). Thus the V-SnO<sub>2</sub> appreciably modifies the transmittance spectrum and the band gap energy value.

## Conclusion

In this work, pure SnO<sub>2</sub> nanoparticles and V-SnO<sub>2</sub> nanocomposites were prepared using sol-gel method and characterized by XRD, SEM and UV-Vis spectroscopic studies. On increasing vanadium content the crystallite size and the intensity of SnO<sub>2</sub> peaks is decreased. The band gap of pure SnO<sub>2</sub> nanoparticles is 3.7 eV which is increased to 3.8 eV for the prepared V-SnO<sub>2</sub> nanocomposites. Thus the addition of vanadium reduces the crystallite size and increases the band gap energy value due to decrease of the size of nanoparticles.

## Acknowledgement

One of the authors (Mohana Priya) sincerely thanks SRM university, Chennai for the award of SRM research fellowship to carryout the work. The authors gratefully acknowledge Prof. D. John Thiruvadigal, Head Department of Physics and Nanotechnology, SRM university for moral support and extending the gratitude (DST-FIST SR/FST/PSI-155/2010) for experimental facilities. The authors also thank Nanotechnology Research Centre, SRM University, Chennai for extending the characterization facilities.

## References

1. Deborah D. L. Chung., Composite materials science and applications, Springer, London Dordrecht Heidelberg NewYork, 2011, 16.
2. Ajayan P M., Schadler L S, Braun P V., Nanocomposite science and technology, wiley- vch verlag GmbH co.k GaA, weinheim, 2003, 9.
3. Gajendran J, Rajendran V., Synthesis and characterization of ultrafine SnO<sub>2</sub> nanoparticles via solvothermal process, Int.J. phy and app, 2010, 2, 45-50.
4. Matthias Batzill , Ulrike Diebold., The surface and materials science of tin oxide, prog surf sci, 2005, 79, 47–154.
5. Sivasankar Reddy A, Figueiredo N M, Cavaleiro A., Nanocrystalline Au: Ag: SnO<sub>2</sub>films prepared by pulsed magnetron sputtering, J Phys. Chem.Solids 2013, 74,825–829.
6. E T H Tan, G W Ho, A S W Wong, S Kawi and A T S Wee., Gas sensing properties of tin oxide nanostructures synthesized via a solid-state reaction method, Nanotechnology,2008, 19, 255-706.
7. Gnanam S, Rajendran V., synthesis of tin oxide nanoparticles by sol- gel process: effect of solvents on the optical properties, J sol-gel sci Technol, 2010, 53,555-559.
8. Xiao Z. R, Guo Y., Structural, electronic and magnetic properties of V<sub>2</sub>O<sub>5-x</sub>: An ab initio study, J. Chem. Phy., 2009,130, 214-704.

9. Darling R. b, and iwanaga S., Structure, properties, and MEMS and microelectronic applications of vanadium oxides, *Sadhana*, 2009, 34, 531–542.
10. Kundu V S, Dhiman V S, Singh D, Maan A S, Arora S., synthesis and characterization of tin oxide nanoparticles via sol-gel method using ethanol as solvent, *ijarse*, 2013, 2, 21-25.
11. Singh A K, Nakate U T., Microwave Synthesis, Characterization and Photocatalytic Properties of SnO<sub>2</sub> Nanoparticles, *Advances in nanoparticles*, 2013, 2 , 66-70
12. Wang C-T, Chen M-T, Lai D-L., Surface characterization and reactivity of vanadium–tin oxide nanoparticles, *App. Surface Science*,2011, 257,5109–5114.
13. Deliang Chen, Lian Gao., Facile synthesis of single-crystal tin oxide nanorods with tunable dimensions via hydrothermal process, *Chem. Phys. Lett.*, 2004, 398,201–206.
14. Si-Dong Kim, Bum-Joon Kim, Jin-Ho Yoon and Jung-Sik Kim., Design, fabrication and characterization of a low-power Gas sensor with high sensitivity to CO gas, *J korean phys. soc.*, 2007,51, 2069-2076.
15. Wang C-T , Chen H-Y, Chen Y-C., Gold/vanadium–tin oxide nanocomposites prepared by co-precipitation method for carbon monoxide gas sensors, *Sensors and Actuators B*, 2013 ,176,945– 951.
16. Psuja P, Hreniak D, Strek W., Synthesis and characterization of indium-tin oxide nanostructures, *Journal of Physics: Conference Series*, 2009, 146, 012033.
17. Baltés M, Cassiers K, Van Der Voort P, Weckhuysen B M, Schoonheydt R A, Vansan E F., MCM-48-Supported Vanadium Oxide Catalysts, Prepared by the Molecular Designed Dispersion of VO(acac)<sub>2</sub>: A Detailed Study of the Highly Reactive MCM-48 Surface and the Structure and Activity of the Deposited VO<sub>x</sub>, *Journal of Catalysis*,2001, 197, 160–171.
18. Dan I. Enache, Elisabeth Bordes-Richard Alain Ensuquea, Francois Bozon-Verduraza, Vanadium oxide catalysts supported on zirconia and titania Preparation and characterization, *Applied Catalysis A: General*,2004, 278,93–102.

\*\*\*\*\*